

Thermodynamic Contribution to the Regulation of Electron Transfer in the Na⁺-Pumping NADH:Quinone Oxidoreductase from *Vibrio cholerae*

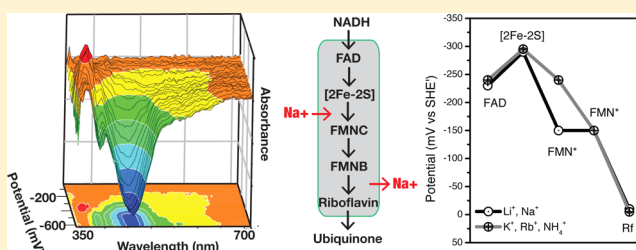
Yashvin Neehaul,[†] Oscar Juárez,[‡] Blanca Barquera,^{*,‡} and Petra Hellwig^{*,†}

[†]Laboratoire de spectroscopie vibrationnelle et électrochimie des biomolécules, Institut de Chimie, UMR 7177, Université de Strasbourg-CNRS, 67070 Strasbourg, France

[‡]Department of Biology, Center for Biotechnology and Interdisciplinary Studies, Rensselaer Polytechnic Institute, Troy, New York 12180, United States

S Supporting Information

ABSTRACT: The Na⁺-pumping NADH:quinone oxidoreductase (Na⁺-NQR) is a fundamental enzyme of the oxidative phosphorylation metabolism and ionic homeostasis in several pathogenic and marine bacteria. To understand the mechanism that couples electron transfer with sodium translocation in Na⁺-NQR, the ion dependence of the redox potential of the individual cofactors was studied using a spectroelectrochemical approach. The redox potential of one of the FMN cofactors increased 90 mV in the presence of Na⁺ or Li⁺, compared to the redox potentials measured in the presence of other cations that are not transported by the enzyme, such as K⁺, Rb⁺, and NH₄⁺. This shift in redox potential of one FMN confirms the crucial role of the FMN anionic radicals in the Na⁺ pumping mechanism and demonstrates that the control of the electron transfer rate has both kinetic (via conformational changes) and thermodynamic components.



The NADH:quinone oxidoreductase (Na⁺-NQR) is a primary Na⁺ pump and the first electron carrier in the respiratory chain of several marine and pathogenic bacteria.^{1–5} This enzyme catalyzes the oxidation of NADH and the reduction of ubiquinone, coupled to the pumping of Na⁺ across the plasma membrane. The Na⁺ gradient is used by bacteria for many vital processes, including ATP synthesis, flagellum rotation, and nutrient uptake. Na⁺-NQR is composed of six subunits (NqrA–F) and contains five redox-active cofactors: an FAD, a [2Fe-2S] center in NqrF, two covalently bound FMN molecules in subunits NqrB and NqrC (FMN_B and FMN_C, respectively), and, remarkably, riboflavin in NqrB.^{6–8} Riboflavin (vitamin B₁₂) is a precursor for the biosynthesis of FAD and FMN, with no participation in enzyme redox chemistry. However, in Na⁺-NQR, riboflavin is a true redox cofactor involved in the electron transfer pathway within the enzyme.^{9,10} This pathway has been described as follows: NADH → FAD → [2Fe-2S] → FMN_C → FMN_B → riboflavin → ubiquinone.⁹

The catalytic mechanism of Na⁺-NQR is still under study, but data indicate that the electron transfer between the different redox centers is coupled to conformational changes in the protein that drive the pumping of sodium.¹¹ Indeed, it has recently been demonstrated that sodium uptake takes place in the step in which an electron moves from the [2Fe-2S] center to FMN_C, while the translocation of sodium across the membrane occurs when one electron is transferred from FMN_B to riboflavin.¹¹ Also, it has been shown that the rate of the redox step involved in sodium capture ([2Fe-2S] →

FMN_C) is the bottleneck reaction of the reduction process and is highly dependent on sodium concentration.^{9,11} Thus, it may be expected that the redox potentials of these cofactors depend on the concentration of the coupling ion (thermodynamic effect) or that the presence of sodium lowers the activation barrier of electron transfer (kinetic effect).¹² Previous studies of the enzyme from *Vibrio haveryi* reported that the redox potentials of all cofactors are independent of the concentration of Na⁺,^{13,14} which suggested that the activation effect could be purely kinetic. In addition, it was reported that the pH-dependent redox transitions (FlH^{•-} ↔ Fl transition of the FAD and the FlH^{•-} ↔ Fl^{•+} transition of FMN_C) are not involved in sodium translocation,¹⁴ which further supports the idea that the coupling is kinetically controlled. In this work, we studied the thermodynamic properties of the redox cofactors of Na⁺-NQR from *Vibrio cholerae* in the presence of Li⁺, Na⁺, K⁺, Rb⁺, and NH₄⁺.

Here we report that the midpoint potential of one of the FMNs is affected by Na⁺ or Li⁺, showing an increase of 90 mV. These results are discussed in the context of how Na⁺ pumping is coupled to the redox reactions of the enzyme.

Received: March 14, 2012

Revised: April 24, 2012

Published: April 25, 2012

MATERIALS AND METHODS

Sample Preparation. Recombinant wild-type Na⁺-NQR, cloned into the pBAD vector and expressed in *V. cholerae* cells, was purified by Ni-NTA affinity chromatography, as described previously.¹⁵ An additional step of cation exchange chromatography was included, using fast flow DEAE-Sepharose, to increase the purity of the sample. After these two purification steps, the protein was washed three times using AMICON centrifugal concentrators (membrane cutoff of 100 kDa) at 6000 rpm with 50 mM Tris-HCl and 0.05% β -D-dodecyl maltoside (pH 8.0) with 150 mM LiCl, NaCl, KCl, RbCl, or NH₄Cl. The final concentration of the enzyme used in most experiments was approximately 0.75 mM.

Redox Titration. Prior to the electrochemical measurements, Na⁺-NQR was mixed with 17 different redox mediators, to a final concentration of 25 μ M in each case, as described previously.¹⁶ For the spectroelectrochemical measurements, a thin layer cell mounted with CaF₂ windows was used.^{17,18} Two gold grids modified with a solution of 2 mM mercaptopropionic acid and 2 mM cysteamine in a 1:1 ratio, laid one over the other, were used as the working electrode. The path length of the sample was \sim 20 μ m. A Ag/AgCl reference electrode was used [add 208 mV for the standard hydrogen electrode (SHE')]. All potentials described hereafter are given versus the SHE', except when described otherwise. During the experiment, the temperature was fixed at 10 °C. The redox-dependent development of the UV-vis signals from 350 to 700 nm was observed with a CARY 300 spectrophotometer that was coupled to a potentiostat. For the electrochemical redox titrations, either the fully oxidized or the fully reduced form of the enzyme was taken as a reference and the spectra were measured between 210 and -410 mV versus the SHE', in 20 mV intervals, with an equilibration time of 40 min for each point. At the end of each titration, the fully oxidized minus reduced difference spectra were compared to the data obtained at the beginning of the experiments to verify the stability of the sample.

Data analysis of the redox-dependent shift of the UV-vis spectra (Δ Abs) is difficult on the basis of a Nernst fit of the redox transition, because the difference spectra of the five-flavin redox transitions and the [2Fe-2S] transition overlap with each other.¹³ Thus, the first derivative of Δ Abs ($\delta\Delta$ Abs) was calculated. The plot of $\delta\Delta$ Abs versus applied potential gave a maximum, which corresponded to the midpoint potential of a redox transition. The different flavins have distinct absorption coefficients, and the contributions of some redox transitions can be neglected at specific wavelengths. All the results were reproducible and fully reversible with an error of \pm 15 mV, estimated from at least three titrations.

RESULTS

The evolution of the redox-dependent absorbance change (Δ Abs) was monitored between 350 and 700 nm (Figure 1). In this range, the four flavins, as well as the [2Fe-2S] center, contribute to the observed spectral changes.⁹ Na⁺-NQR contains a tightly bound ubiquinone,¹⁹ which does not participate in the redox process, as observed in previous studies⁹ and in our spectroelectrochemical approach. The molar absorption coefficients of the six observable transitions in this interval were reported previously.⁹ On this basis, the spectral changes at 560, 460, and 380 nm were selected for data analysis as all the contribution from the different cofactors can be

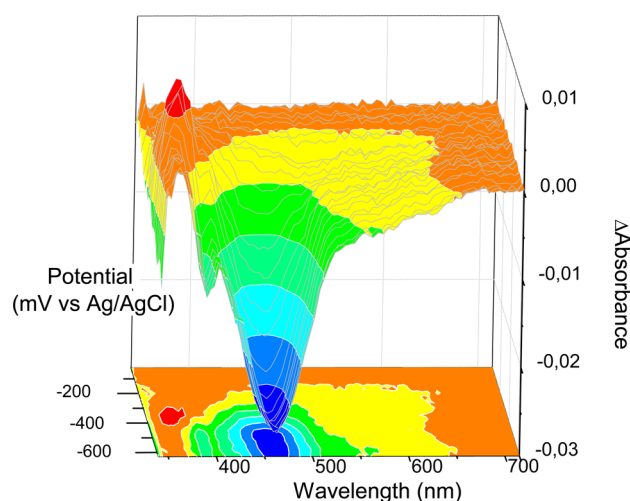


Figure 1. Evolution of the difference spectra upon performance of a reductive titration of Na⁺-NQR. Δ Abs values at 460, 560, and 380 nm were used for data analysis.

inferred. Figure 2 shows the plot at 560, 460, and 380 nm of the first derivative of Δ Abs versus the applied potential in the presence of Li⁺, Na⁺, K⁺, Rb⁺, or NH₄⁺.

At 380 nm, the signals of the FIH⁻ \leftrightarrow FI transition from FAD ($\epsilon_{\text{red-ox}} = -4.25 \text{ mM}^{-1} \text{ cm}^{-1}$) and the FIH⁻ \leftrightarrow FI[•] transition of FMN_C ($\epsilon_{\text{red-ox}} = -6.95 \text{ mM}^{-1} \text{ cm}^{-1}$) are predominant and can be studied with minimal interference from other transitions. Figure 2 shows that in the presence of Na⁺ or Li⁺ a single peak was found, with a midpoint potential of -230 mV (Table 1). The single peak clearly indicates that midpoint potentials of the two-electron transition of FAD (FIH⁻ \leftrightarrow FI) and the one-electron transition of FMN_C (FIH⁻ \leftrightarrow FI[•]) are very close and cannot be separated. Figure 2 also shows that in the presence of K⁺, Rb⁺, and NH₄⁺, a small downshift in this peak of 25 mV was observed.

At 560 nm, the one-electron transitions [2Fe-2S]²⁺ \leftrightarrow [2Fe-2S]^{2•} ($\epsilon_{\text{red-ox}} = -1.54 \text{ mM}^{-1} \text{ cm}^{-1}$) and FIH⁻ \leftrightarrow FI[•] ($\epsilon_{\text{red-ox}} = -1.4 \text{ mM}^{-1} \text{ cm}^{-1}$) from FMN_C and the transition FIH⁻ \leftrightarrow FIH₂ ($\epsilon_{\text{red-ox}} = -3.84 \text{ mM}^{-1} \text{ cm}^{-1}$) from riboflavin have the most intense contributions. The contribution of the FIH⁻ \leftrightarrow FI[•] transition from FMN_C, however, is practically canceled by the FIH⁻ \leftrightarrow FI transition from FAD, because these two transitions appear concurrently and the contribution of FAD is negative ($\epsilon_{\text{red-ox}} = 1.1 \text{ mM}^{-1} \text{ cm}^{-1}$). At this wavelength, two redox potentials were observed at -300 and -10 mV, showing no dependence on the ion used in the experiment. The potential at -300 mV corresponds to the [2Fe-2S] center and the potential at -10 mV to riboflavin.

Finally, at 460 nm, the two-electron FIH⁻ \leftrightarrow FI transition of FAD ($\epsilon_{\text{red-ox}} = -11.2 \text{ mM}^{-1} \text{ cm}^{-1}$) and the FI[•] \leftrightarrow FI transition ($\epsilon_{\text{red-ox}} = -8.8 \text{ mM}^{-1} \text{ cm}^{-1}$) from both FMN_B and FMN_C can be expected. Although other transitions contribute to the absorption at this wavelength, their molar absorption coefficients are small. Interestingly, the different midpoint components studied at this wavelength were dependent on the ion used in the experiment. In the presence of Li⁺ or Na⁺ ions, two maxima are observed at -240 and -150 mV. The half-widths of these peaks correspond to 41 and 168 mV, respectively, suggesting a two-electron transition for the peak at -240 mV and two one-electron transitions for the peak at -150 mV. Data were fit to a three-component Gaussian model; one component had a fixed half-width of 45 mV (correspond-

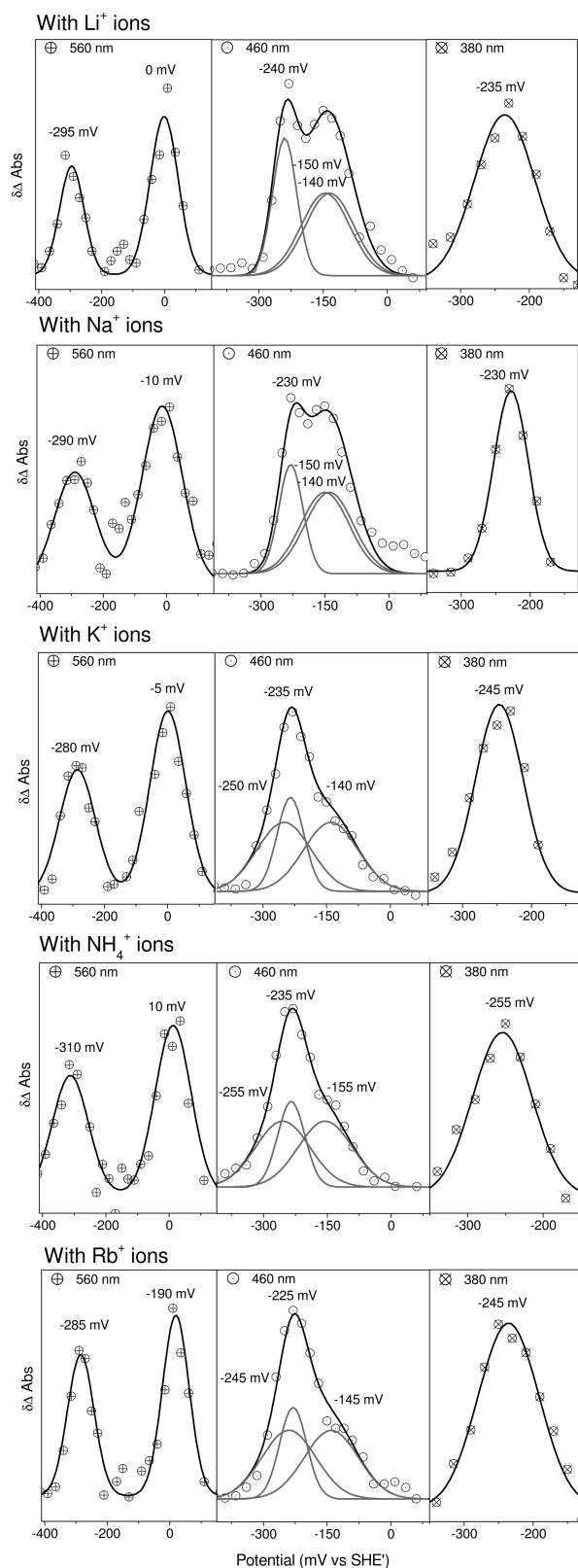


Figure 2. Example of redox titration of Na⁺-NQR from *V. cholerae*. $\delta\Delta\text{Abs}$ values at 560, 460, and 380 nm with Li⁺, Na⁺, K⁺, Rb⁺, or NH₄⁺. The maxima correspond to the midpoint potentials of the cofactors involved. Data were fit to a Gaussian model with fixed bandwidths of 45 and 90 mV for one and two-electron transitions, respectively.

ing to the FIH[−] ↔ FI transition of FAD), and the other two components had the same intensity and a half-width of 90 mV (corresponding to the FI^{•−} ↔ FI transition from FMN_B and FMN_C). These findings led to the conclusion that the peak at −240 mV corresponds to the FAD FIH[−] ↔ FI transition and that the peak at −150 mV contains the contributions of the FI^{•−} ↔ FI transition of the two FMNs. The redox potentials of the FI^{•−} ↔ FI transition of the two FMNs cannot be unequivocally discriminated, because the values are too close to each other (<40 mV). In the presence of K⁺ or Rb⁺, the plot of $\delta\Delta\text{Abs}$ versus the potential shows a decrease in intensity for the peak at −150 mV and an increase in intensity for the peak at −240 mV; the latter also becomes broader. A three-component fit shows that the peak attributed to FAD with a half-width of 45 mV is not altered. For the two FI^{•−} ↔ FI transitions of the FMNs, a component remains unchanged at −140 mV and the other is downshifted by 90 mV to −230 mV. These findings suggest that the FAD FIH[−] ↔ FI transition at −240 mV and one of the FMN FI^{•−} ↔ FI transitions with a redox potential of −150 mV are not dependent on the ion present, but one of the redox potentials of the FI^{•−} ↔ FI transition of the FMN centers is modulated by Na⁺ or Li⁺.

To corroborate the assignments made by the analysis of the plots of $\delta\Delta\text{Abs}$ versus the potential, we obtained differential spectra at specific potential ranges and compared those spectra with the spectra of the redox transitions characterized previously. Figure 3 shows the differential spectra of wild-type Na⁺-NQR in the presence of Na⁺ and K⁺. Consistent with the data in Table 1, the spectra between −70 and 160 mV with Na⁺ and K⁺ showed a strong contribution of the FIH[−] ↔ FIH₂ transition from riboflavin, with minima at 525 and 560 nm and a maximum at 430 nm. The differential spectra obtained from −190 to −70 mV showed a minimum at 460 nm, corresponding to the FI^{•−} ↔ FI transition. As expected, in the presence of sodium, two FMN molecules were found, and only one with potassium. The differential spectra from −410 to −190 mV showed the contributions of the FAD (FIH[−] ↔ FI), the FIH[−] ↔ FI^{•−} transition of FMN_C, and the [2Fe-2S] center. When K⁺ is used, the differential spectra from −410 to −190 mV include the contributions of FAD (FIH[−] ↔ FI), the FIH[−] ↔ FI^{•−} transition from FMN_C, and the [2Fe-2S] center (minima at 390 and 460 nm and a small contribution between 500 and 575 nm). In the presence of sodium, these transitions were accompanied by the FI^{•−} ↔ FI transition from a single FMN (the minimum at 460 nm is lower than the minimum at 390 nm). The plot of $\delta\Delta\text{Abs}$ versus applied potential in the presence of Na⁺ and K⁺ ions for each 5 nm step from −350 to 600 nm is shown in Figure 4. The maximum at −360 mV in the presence of Na⁺ is decreased when K⁺ is present. Furthermore, the peak at −440 mV becomes broader in the presence of Na⁺, showing the observed shift in potential. Analogous plots for Li⁺, Rb⁺, and NH₄⁺ are shown in Figure 1 of the Supporting Information.

DISCUSSION

The electron transfer pathway in Na⁺-NQR is composed of four flavins and a [2Fe-2S] center. The iron–sulfur center connects the two-electron reaction of the FAD with the one-electron module in the enzyme, composed by the two covalently bound FMNs and riboflavin, which are involved in sodium translocation.¹¹

The cycle begins with the transfer of two electrons from NADH to FAD. After this step, the electrons are split,

Table 1. Midpoint Potentials of the Cofactors in Na⁺-NQR from *V. cholerae* in the Presence of Different Ions (average from three titrations)

cofactor	redox transition	no. of electrons	E_m (mV vs SHE')				
			Li ⁺	Na ⁺	K ⁺	Rb ⁺	NH ₄ ⁺
FAD	FlH [•] ↔ Fl	2	−235	−230	−240	−235	−230
[2Fe-2S]	[2Fe-2S] ^{•+} ↔ [2Fe-2S] ²⁺	1	−300	−290	−290	−300	−300
FMN _{C/B}	Fl [•] ↔ Fl	1	−140/−150	−135/−150	−150/−240	−135/−250	−135/−240
FMN _C	FlH [•] ↔ Fl [•]	1	−230	−230	−255	−255	−250
riboflavin	FlH [•] ↔ FlH ₂	1	0	−5	−10	0	5

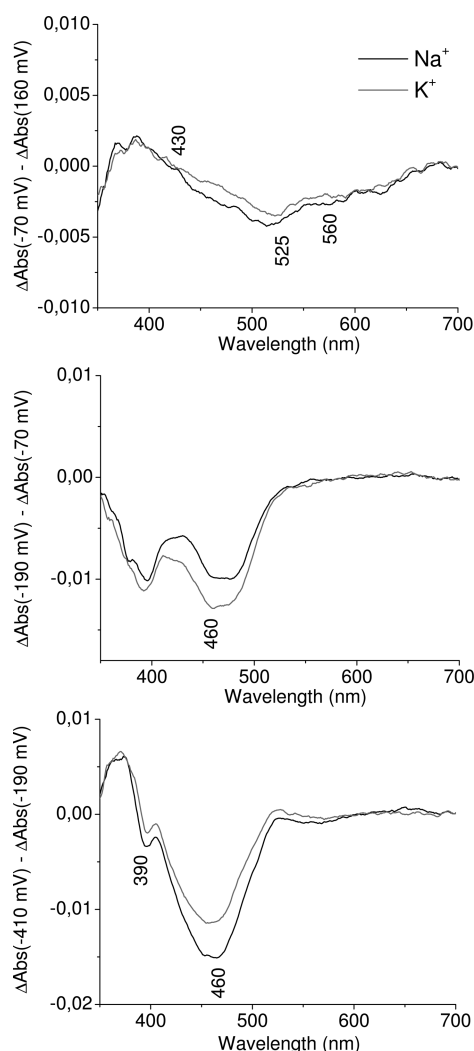


Figure 3. Differential plot in the presence of Na⁺ (black) and K⁺ (gray) of ΔAbs at −70 mV minus 160 mV (top), ΔAbs at −190 mV minus −70 mV (middle), and ΔAbs at −410 mV minus −190 mV (bottom).

producing the fully reduced [2Fe-2S] center and an unstable FAD semiquinone radical.²⁰ Electrons then are transferred to FMN_C and FMN_B, producing anionic radicals, and finally delivered to riboflavin.⁹ Riboflavin is the final electron carrier in the enzyme⁷ and delivers electrons to ubiquinone. Interestingly, riboflavin is found as a stable neutral radical in the oxidized state of the enzyme.^{7,10}

Several models discuss the role of the flavin semiquinone radicals in the mechanism of Na⁺-NQR.¹² In most of these models, the transfer of electron to the flavins, with the

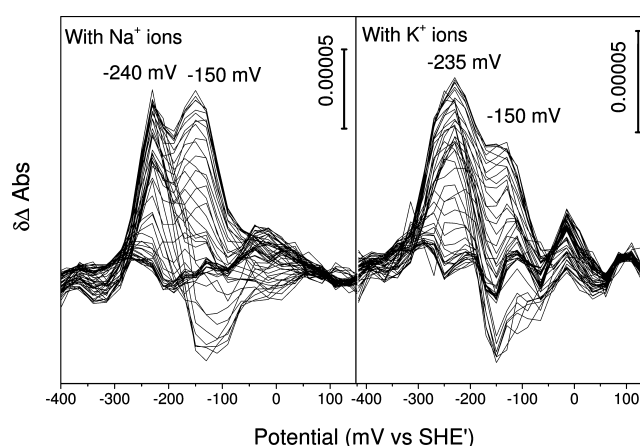


Figure 4. Plots of δΔAbs vs the applied potential for each 5 nm from 350 to 600 nm with Na⁺ (left) and K⁺ (right).

concomitant production of a negative charge, was suggested to be directly connected to the electroneutral uptake of sodium, through a thermodynamic coupling.^{21,22} In these models, the affinity of the pumped ions would be modified by the redox state of the enzyme, and the midpoint potential of the redox cofactor involved in sodium translocation would be dependent on the concentration of the cation, in a ratio of 60 mV/pNa. However, our work has demonstrated that the mechanism of sodium pumping involves two redox transitions, and no single cofactor is involved in sodium uptake and release, which indicates that the coupling mechanism is not direct and could be kinetically controlled; the conformational changes during the translocation of sodium presumably reduce the activation barrier of electron transfer between the redox centers.^{11,23}

In this work, we have examined the dependence of different ions on the midpoint potentials of the redox cofactors of Na⁺-NQR, to clarify the thermodynamic contributions in the process of electron transfer. Recently, it has also been shown that Na⁺-NQR can use either Li⁺ or Na⁺ as a substrate, and that K⁺ acts as an activator that modulates the affinity of the enzyme for sodium. Rb⁺ competes for potassium for its binding site but acts as an inhibitor.²³ The redox titrations were performed in the presence of either coupling ion (Na⁺ or Li⁺), and also in the presence of ions that cannot be transported by the enzyme. (K⁺, Rb⁺, or NH₄⁺).

The midpoint potential of a Fl[•] ↔ Fl transition of one of the FMN cofactors increases 90 mV in the presence of sodium or lithium, but not with potassium, rubidium, or ammonium (E_m of −150 mV in the presence of Li⁺ and Na⁺ vs −230 mV in the presence of K⁺, Rb⁺, and NH₄⁺). Meanwhile, the midpoint potential of the other cofactors remained largely unperturbed. These results corroborate that the one-electron reduction of one FMN is crucial for the transfer of ion across the membrane.

On the basis of the electron transfer pathway, we suggest that FMN_C is the sodium-dependent group, because its reduction is involved in sodium capture. FMN_C is localized in the soluble cytoplasmic domain of NqrC, covalently binding to threonine in NqrC by phosphoester bonds.^{24–26} The results are summarized in Table 1, and the scheme of electron transfer with respect to the energy level of each cofactor is shown in Figure 5.

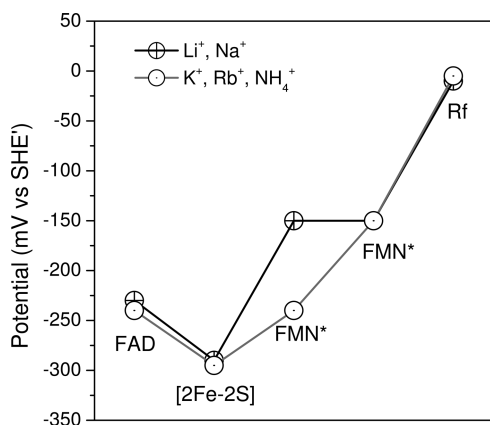


Figure 5. Energy levels of the different cofactors involved in electron transfer with the different ions. The FMN* redox potential corresponds to the $\text{Fl}^{\bullet-} \leftrightarrow \text{Fl}$ transition of either FMN_C or FMN_B. A clear shift is observed upon comparison of the presence of Na⁺ and K⁺.

Previously, the midpoint potential of the $\text{Fl}^{\bullet-} \leftrightarrow \text{Fl}$ transition of the two FMN cofactors, measured in the enzyme from *V. harveyi*, was found to be independent of the presence of sodium, with midpoint potentials of -200 mV for FMN_C and -130 mV for FMN_B.¹⁴ We cannot infer the reason of such a large difference in the behavior of the enzymes from *V. cholerae* versus *V. harveyi*. However, our preparation has the largest sodium-sensitive activity reported so far (140 units/mg of protein), a high purity (>95%), and a sodium or lithium pumping activity when the enzyme is reconstituted into proteoliposomes.^{7,23} Also, the activity of the recombinant enzyme is able to rescue the deletion strain of *nqr*, when these cells, expressing Na⁺-NQR, are grown in the presence of the uncoupler CCCP (unpublished results), indicating that Na⁺-NQR is fully functional.

Here we show that the presence of sodium or lithium produces a large increase in the midpoint potential of a single FMN, which could account for the stimulation of the activity by the two cations. This also suggests that the coupling mechanism is thermodynamically influenced and that presumably works together with kinetic mechanisms to regulate the electron transfer rate of the enzyme. Interestingly, it was previously shown that the affinity of Na⁺-NQR for sodium does not change between the fully oxidized and fully reduced states of the enzymes.²³ The results indicate that while sodium regulates the midpoint potential of FMN, the redox state of the enzyme does not regulate sodium affinity. This clearly indicates that Na⁺-NQR does not operate through a true redox Bohr effect, and thus, it does not behave according to thermodynamic box models, like the ones proposed by Wyman²⁷ and Wikström.²⁸ The lack of a redox Bohr effect demonstrates that the coupling mechanism of the enzyme is not localized and that the sodium binding pocket is physically separated from the electron transfer

machinery, which explains the lack of reciprocal effects between sodium binding and redox events.

Even though the two coupling ions produce a large change in the midpoint potential of one FMN, the kinetic mechanism seems to have a role as the rate-limiting step: while saturating concentrations of both sodium and lithium produce the same decrease in the midpoint potential of the FMN cofactor, sodium stimulates the activity 8-fold, while lithium stimulates the activity only 3-fold.²³ The net coupled activity [total activity minus the uncoupled activity (activity without ions)] with sodium and lithium as substrates is around 440 and 120 s⁻¹, respectively.²³ This strongly suggests that, although there are thermodynamic factors that regulate the electron transfer in Na⁺-NQR, the control is exerted by kinetic factors, probably through conformational changes.

■ ASSOCIATED CONTENT

§ Supporting Information

Plot of ΔAbs versus applied potential of Na⁺-NQR in the presence of Li⁺, Na⁺, K⁺, Rb⁺, and NH₄⁺ ions in 5 nm steps from 350 to 600 nm. The plots obtained in the presence of Li⁺ and Na⁺ ions are similar. In the presence of K⁺, Rb⁺, and NH₄⁺, the plot depicts the change in potential of one of the cofactors, which corresponds to FMN, as explained in the text. This material is available free of charge via the Internet at <http://pubs.acs.org>.

■ AUTHOR INFORMATION

Corresponding Author

*Laboratoire de spectroscopie vibrationnelle et électrochimie des biomolécules, Institut de Chimie, UMR 7177, Université de Strasbourg-CNRS, 1 Rue Blaise Pascal, 67070 Strasbourg, France. Telephone: 00 33 3 68 85 12 73. Fax: 00 33 3 68 85 14 31. E-mail: hellwig@unistra.fr.

Funding

P.H. and Y.N. are grateful for the financial support by the ANR chaire d'excellence, the French ministry for research and higher education, and the CNRS. B.B. and O.J. acknowledge support from National Science Foundation Grant MCB 1052234 and National Institutes of Health Grant GM 060036.

Notes

The authors declare no competing financial interest.

■ ACKNOWLEDGMENTS

We thank Dr. Antoine Bonnefont (Université de Strasbourg) for helpful discussions.

■ ABBREVIATIONS

Na⁺-NQR, Na⁺-pumping NADH:quinone oxidoreductase; Fl, oxidized flavin; FlH⁻, anionic reduced flavin; FlH[•], neutral flavosemiquinone; FlH₂, neutral reduced flavin; Fl^{•-}, anionic flavosemiquinone; ΔAbs , difference in absorbance; $\delta\Delta\text{Abs}$, first derivative of ΔAbs .

■ REFERENCES

- (1) Häse, C. C., and Barquera, B. (2001) Role of sodium bioenergetics in *Vibrio cholerae*. *Biochim. Biophys. Acta* 1505, 169–178.
- (2) Unemoto, T., and Hayashi, M. (1993) Na⁺-translocating NADH-quinone reductase of marine and halophilic bacteria. *J. Bioenerg. Biomembr.* 25, 385–392.
- (3) Kogure, K. (1998) Bioenergetics of marine bacteria. *Curr. Opin. Biotechnol.* 9, 278–282.

- (4) Steuber, J. (2001) Na⁺ translocation by bacterial NADH:quinone oxidoreductases: An extension to the complex-I family of primary redox pumps. *Biochim. Biophys. Acta* 1505, 45–56.
- (5) Kerscher, S., Dröse, S., Zickermann, V., and Brandt, U. (2008) The three families of respiratory NADH dehydrogenases. In *Results and Problems in Cell Differentiation* (Differ, R. P. C., Ed.) pp 185–222, Springer, New York.
- (6) Barquera, B., Zhou, W., Morgan, J. E., and Gennis, R. B. (2002) Riboflavin is a component of the Na⁺-pumping NADH:quinone oxidoreductase from *Vibrio cholerae*. *Proc. Natl. Acad. Sci. U.S.A.* 99, 10322–10324.
- (7) Juárez, O., Nilges, M. J., Gillespie, P., Cotton, J., and Barquera, B. (2008) Riboflavin is an active redox cofactor in the Na⁺-pumping NADH:quinone oxidoreductase (Na⁺-NQR) from *Vibrio cholerae*. *J. Biol. Chem.* 283, 33162–33167.
- (8) Casutt, M. S., Huber, T., Brunisholz, R., Tao, M., Fritz, G., and Steuber, J. (2010) Localization and function of the membrane-bound riboflavin in the Na⁺-translocating NADH:quinone oxidoreductase (Na⁺-NQR) from *Vibrio cholerae*. *J. Biol. Chem.* 285, 27088–27099.
- (9) Juárez, O., Morgan, J. E., and Barquera, B. (2009) The electron transfer pathway of the Na⁺-pumping NADH:quinone oxidoreductase from *Vibrio cholerae*. *J. Biol. Chem.* 284, 8963–8972.
- (10) Barquera, B., Ramirez-Silva, L., Morgan, J. E., and Nilges, M. J. (2006) A new flavin radical signal in the Na⁺-pumping NADH:quinone oxidoreductase from *Vibrio cholerae*. An EPR/electron nuclear double resonance investigation of the role of the covalently bound flavins in subunits B and C. *J. Biol. Chem.* 281, 36482–36491.
- (11) Juárez, O., Morgan, J. E., Nilges, M. J., and Barquera, B. (2010) Energy transducing redox steps of the Na⁺-pumping NADH:quinone oxidoreductase from *Vibrio cholerae*. *Proc. Natl. Acad. Sci. U.S.A.* 107, 12505–12510.
- (12) Bogachev, A. V., and Verkhovsky, M. I. (2005) Na⁺-Translocating NADH:quinone oxidoreductase: Progress achieved and prospects of investigations. *Biochemistry (Moscow, Russ. Fed.)* 70, 143–149.
- (13) Bogachev, A. V., Bertsova, Y. V., Bloch, D. A., and Verkhovsky, M. I. (2006) Thermodynamic properties of the redox centers of Na⁺-translocating NADH:quinone oxidoreductase. *Biochemistry* 45, 3421–3428.
- (14) Bogachev, A. V., Bloch, D. A., Bertsova, Y. V., and Verkhovsky, M. I. (2009) Redox properties of the prosthetic groups of Na⁺-translocating NADH:quinone oxidoreductase. 2. Study of the enzyme by optical spectroscopy. *Biochemistry* 48, 6299–6304.
- (15) Barquera, B., Hellwig, P., Zhou, W., Morgan, J. E., Hase, C. C., Gosink, K. K., Nilges, M., Bruesehoff, P. J., Roth, A., Lancaster, C. R., and Gennis, R. B. (2002) Purification and characterization of the recombinant Na⁺-translocating NADH:quinone oxidoreductase from *Vibrio cholerae*. *Biochemistry* 41, 3781–3789.
- (16) Behr, J., Hellwig, P., Mäntele, W., and Michel, H. (1998) Redox dependent changes at the heme propionates in cytochrome *c* oxidase from *Paracoccus denitrificans*: Direct evidence from FTIR difference spectroscopy in combination with heme propionate ¹³C labeling. *Biochemistry* 37, 7400–7406.
- (17) Moss, D., Nabedryk, E., Breton, J., and Mäntele, W. (1990) Redox-linked conformational changes in proteins detected by a combination of infrared spectroscopy and protein electrochemistry. Evaluation of the technique with cytochrome *c*. *Eur. J. Biochem.* 187, 565–572.
- (18) Hellwig, P., Ostermeier, C., Michel, H., Ludwig, B., and Mantele, W. (1998) Electrochemically induced FT-IR difference spectra of the two- and four-subunit cytochrome *c* oxidase from *P. denitrificans* reveal identical conformational changes upon redox transitions. *Biochim. Biophys. Acta* 1409, 107–112.
- (19) Casutt, M. S., Nediakov, R., Wendelspiess, S., Vossler, S., Gerken, U., Murai, M., Miyoshi, H., Möller, H. M., and Steuber, J. (2011) Localization of ubiquinone-8 in the Na⁺-pumping NADH:quinone oxidoreductase from *Vibrio cholerae*. *J. Biol. Chem.* 286, 40075–40082.
- (20) Bogachev, A. V., Belevich, N. P., Bertsova, Y. V., and Verkhovsky, M. I. (2009) Primary steps of the Na⁺-translocating NADH:ubiquinone oxidoreductase catalytic cycle resolved by the ultrafast freeze-quench approach. *J. Biol. Chem.* 284, 5533–5538.
- (21) Rich, P. R., Meunier, B., and Ward, F. B. (1995) Predicted structure and possible ionmotive mechanism of the sodium-linked NADH-ubiquinone oxidoreductase of *Vibrio alginolyticus*. *FEBS Lett.* 375, 5–10.
- (22) Dimroth, P. (1997) Primary sodium ion translocating enzymes. *Biochim. Biophys. Acta* 1318, 11–51.
- (23) Juárez, O., Shea, M. E., Makhadze, G. I., and Barquera, B. (2011) The role and specificity of the catalytic and regulatory cation-binding sites of the Na⁺-pumping NADH:quinone oxidoreductase from *Vibrio cholerae*. *J. Biol. Chem.* 286, 26383–26390.
- (24) Barquera, B., Hase, C. C., and Gennis, R. B. (2001) Expression and mutagenesis of the NqrC subunit of the NQR respiratory Na⁺ pump from *Vibrio cholerae* with covalently attached FMN. *FEBS Lett.* 492, 45–49.
- (25) Hayashi, M., Nakayama, Y., Yasui, M., Maeda, M., Furuishi, K., and Unemoto, T. (2001) FMN is covalently attached to a threonine residue in the NqrB and NqrC subunits of Na⁺-translocating NADH-quinone reductase from *Vibrio alginolyticus*. *FEBS Lett.* 488, 5–8.
- (26) Nakayama, Y., Yasui, M., Sugahara, K., Hayashi, M., and Unemoto, T. (2000) Covalently bound flavin in the NqrB and NqrC subunits of Na⁺-translocating NADH-quinone reductase from *Vibrio alginolyticus*. *FEBS Lett.* 474, 165–168.
- (27) Wyman, J. (1968) Regulation in macromolecules as illustrated by haemoglobin. *Q. Rev. Biophys.* 1, 35–80.
- (28) Krab, K., and Wikström, M. (1979) On the stoichiometry and thermodynamics of proton-pumping cytochrome *c* oxidase in mitochondria. *Biochim. Biophys. Acta* 548, 1–15.